Computer & Robotics

A Robust Optimization Framework for Energy Management in Energy Hubs: Comparative Analysis of SMA, GA, and MILP with Demand Response Integration

Mohammad Reza Ohadi[1], Mahdi Hedayati[1,*], Reza Effatnejad[1], Abdolreza Dehghani Tafti[1]

[1]*Department of Electrical Engineering, Karaj Branch, Islamic Azad University, Karaj, Iran*

Received 11 September 2024, Accepted 09 November 2024

Abstract

This study presents a combined energy system (CES) framework for optimizing energy management in energy hubs (EHs), incorporating renewable energy sources (RERs) and demand response (DR) programs. Uncertainties in wind, solar, and energy prices are managed using a stochastic scenario-based approach. We compare the performance of three optimization techniques: Slime Mould Algorithm (SMA), Genetic Algorithm (GA), and Mixed-Integer Linear Programming (MILP). SMA consistently demonstrates superior cost-effectiveness, reducing operational costs by up to 10% compared to GA and MILP. With DR integration, SMA further decreases costs, highlighting its efficiency in enhancing renewable energy utilization. These results affirm the potential of SMA as a robust and reliable solution for modern energy systems.

Keywords: Energy management, Renewable energy sources, Demand response programs, Slime Mould Algorithm (SMA), Mixed-Integer Linear Programming (MILP), Genetic Algorithm

1.Introduction

Growing energy demand and environmental challenges have accelerated reliance on distributed energy resources (DERs), energy storage systems (ESs), and demand response (DR) initiatives, with renewable energy sources (RES) at the core of clean energy generation [1]. Microgrids, integrating distributed generations (DGs), ESs, and responsive loads, address the grid stability challenges posed by RES variability by functioning both in grid-connected and islanded modes [2,3]. Combining ESs and responsive loads with RES-based DGs within microgrids enhances reliability and balances generation with demand, reducing operational costs and emissions while supporting DR programs [4]. Interconnected microgrids, or networked microgrids (NMGs), further improve system performance and reliability, enabling economic dispatch and power exchange among microgrids for resilient and cost-effective power supply [5-7].

However, adopting networked microgrids (NMGs) requires an active energy management system (EMS) to optimize operational costs, reliability, and environmental performance [8]. An EMS manages dispatchable DGs (e.g., microturbines), ESs, demand-side management, and power exchanges among microgrids [9]. With increasing RES integration, probabilistic models have become essential to address uncertainties that deterministic methods cannot handle [10]. In addition, optimization methods such as Mixed-Integer Linear Programming (MILP) are widely used for managing continuous and discrete variables in energy management. This study introduces the Slime Mould Algorithm (SMA) and compares it with the Genetic Algorithm (GA) and MILP, highlighting SMA's advantages in efficient and cost-effective energy management [11].

1.1. Related Research Background

Research on Networked Microgrid (NMG) operations has proposed strategies to enhance resilience, economic dispatch, and cost-effective scheduling. For instance, a recent study introduced a nested energy management strategy for NMG day-ahead scheduling, achieving efficient and economical operations, though without addressing uncertainties in RES outputs [12].

[*]Corresponding Author. Email: m.hedayati@ kiau.ac.ir

A Software-Defined Networking (SDN) architecture was proposed in [13] to enhance resilience and efficiency by networking isolated microgrids for rapid power support. However, deterministic approaches in [14] did not address uncertainties. Decentralized economic dispatch methods, involving collaboration between the distribution system operator (DSO) and microgrid central controllers, have also been explored for energy optimization, though without assessing demand response (DR) impacts on scheduling [15]. A hierarchical stochastic EMS for interconnected microgrids was proposed in [16], introducing probabilistic control for power exchanges with the main grid, although power pricing between microgrids was not considered.

A decentralized EMS was developed for optimal NMG operation within distribution systems, treating distribution operators and microgrid controllers as independent entities with cost-minimization objectives, though without detailing power exchange pricing calculations [17]. Other studies have examined demand response programs (DRP) in microgrid networks. For instance, [18] proposed a two-period stochastic programming framework for optimizing investment and operation in a single microgrid with energy storage (ES) and DRP but did not address interconnected microgrid structures. In multi-carrier NMGs, a probabilistic analysis explored optimal load dispatch under RES and load uncertainties, incorporating demand-side management to mitigate peak consumption [19].

In [20], a survivability-oriented demand response program (DRP) was proposed, using robust optimization to address uncertainties in renewable energy sources (RES) and loads, aiming to minimize load shedding. An optimal scheduling problem for NMGs under RES and load uncertainties was introduced in [21], integrating time-of-use (TOU) and real-time pricing (RTP) DRPs and solving it with a metaheuristic algorithm. Additionally, a bargaining-based energy trading market for interconnected microgrids was developed in [22] to optimize energy exchanges and costs, though it did not account for uncertainties in RES or load consumption.

The optimal operation of reconfigurable distribution systems with multiple microgrids was explored in [23], incorporating DRP and energy storage (ES) under uncertainty, with power exchange costs estimated based on day-ahead market prices. Robust optimization methods for managing microgrid operations in the presence of RES were further developed in [24], suggesting reactive loads to handle wind and solar variability. Additionally, a game-theory-based DR program (GTDR) was introduced in [25] to optimize microgrid dispatch, reducing costs and load levels. In [26], a modified particle swarm optimization (PSO) algorithm was applied for real-time energy management to optimize battery operations, while a multi-objective scheduling model using DR was proposed for cost-effective management of CCHP microgrids [27].

Probabilistic multi-objective operation planning for smart distribution systems was discussed in [28], focusing on optimal operations with distributed generation (DG) sources and reactive loads. Scheduling renewables and demand response in a sub-grid was examined in [29], though emissions and grid exchanges were not considered. Intelligent energy management systems, incorporating both electricity and heat production, were introduced for comprehensive load coverage in microgrids [30]. Additionally, a multi-purpose microgrid operation, including wind, solar, fuel cells, and storage, was optimized to minimize costs and pollution [31]. A chance-constrained programming approach for hybrid microgrids addressed uncertainties in RES and market prices to reduce costs [32].

A fuzzy programming approach was used in [33] to address uncertainties in microgrid scheduling. Various methods have been developed to model uncertainties from renewable energy sources, primarily differing in how input uncertainties are represented [34]. For instance, a probabilistic framework utilizing the point estimate method was applied in [35] to model uncertainties in RES, electricity prices, and load demand. Additionally, a hybrid forecasting model combining wavelet transform and a neural network was proposed to predict solar energy in PV-PHES systems with demand response [36]. Probabilistic methods, which assess renewable energy impacts more effectively, use probability density functions (PDF) for demand response, solar generation, and market prices to model variability, with standard deviation based on probability differences [37].

Mixed-Integer Linear Programming (MILP) is extensively used in microgrid energy management for handling both continuous and discrete variables. For example, MILP has been applied to optimize microgrid operations under constraints and uncertainties, demonstrating its effectiveness in integrating renewable energy sources and demand response [38]. Additionally, MILP has proven efficient for scheduling distributed energy resources and minimizing operational costs in renewable-integrated microgrids [39]. To evaluate optimization methods for complex energy management, this study compares the Slime

Mould Algorithm (SMA) with Genetic Algorithm (GA) and MILP, highlighting SMA's advantages in efficient, cost-effective energy management.

1.2. Key Contributions

The uncertain generation of wind and photovoltaic (PV) power, along with the complexities of power flow analysis, have often been overlooked in recent literature. To address these gaps, this study presents a scenario-based stochastic optimization framework designed to manage uncertainties and optimize energy management in energy hubs (EHs). The framework integrates industrial, commercial, and residential participants, along with both controllable and non-controllable appliances, to maximize the operational efficiency and cost-effectiveness of EHs.
The major contributions of this study are as follows:

- **Integration of Demand Response (DR) Programs**: This study incorporates a DR program that enhances energy management flexibility. This approach allows for efficient utilization of energy resources by shifting and managing loads to minimize losses and improve overall performance. The thermal model adapts power profiles of thermostatically controllable loads, maintaining required temperature ranges.

- **Comprehensive Uncertainty Modelling**: The framework effectively models the uncertainties associated with renewable energy sources (RES) such as wind and PV. This comprehensive uncertainty modelling ensures a more reliable and accurate energy management strategy, accommodating the inherent variability in RES generation.

- **Optimization Algorithms**: The study utilizes the Slime Mould Algorithm (SMA) and compares its performance with the Genetic Algorithm (GA) and Mixed-Integer Linear Programming (MILP) to evaluate their effectiveness in minimizing operational costs and maximizing the utilization of renewable energy sources.

- **Scenario-Based Energy Management System (EMS)**: The proposed stochastic model is validated through simulation under several case studies, comparing its performance with a deterministic method. The results demonstrate the effectiveness of the scenario-based EMS framework in optimizing the operation of multi-component EHs, highlighting its superiority in managing uncertainties and improving energy efficiency.

1.3. Organization of the Paper

The remainder of the paper is organized as follows: Section 2 presents the general scheme of the proposed framework, detailing the assumed energy hub structure and the various components involved. Section 3 outlines the mathematical problem formulation, including objective functions and constraints for different components such as CHP units, gas boilers, ESS, thermal energy storage, and DR programs. Section 4 discusses the simulation results and performance comparison using the Slime Mould Algorithm (SMA) and Genetic Algorithm (GA). Finally, Section 5 draws the conclusions, summarizing the findings and providing suggestions for future research.

2. General scheme of the Proposed Framework

The energy hub is designed to be supplied by photovoltaic (PV) systems, wind turbines (WT), combined heat and power (CHP) units, the natural gas network, and the electricity grid. Due to the lack of economic justification for batteries in a grid-connected system, they are not included in the current model. Instead, any excess electricity generated is sold back to the grid.
The demand side of the hub includes electrical, heating, and cooling loads. Heating demand is met by a combination of a natural gas-fuelled boiler and CHP units. Cooling demand is addressed through the use of both absorption chillers and electric chillers, with the absorption chillers also requiring their own heating input.
Electricity demand is met by both the grid and the CHP system. This integrated approach ensures that the energy hub can efficiently manage and optimize the supply and demand of multiple energy sources.
A schematic representation of the described energy hub structure is illustrated in **Figure 1** This diagram provides a visual overview of the energy flows and components within the hub, highlighting the interconnected nature of the system.

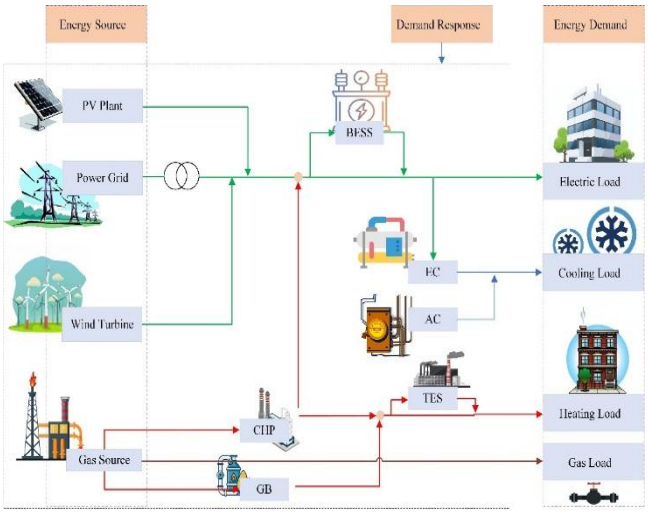

Fig. 1. Structure of Hybrid integrated energy systems.

3. Mathematical Problem Formulation

3.1. Objective Functions

The primary objective of the proposed scheduling for a multi-carrier energy system, based on the energy hub (EH) concept, is to minimize the operation cost for the EH operator. This objective is mathematically formulated in Equation (1). The objective function consists of six terms, each representing a different cost component associated with the operation of the EH.

The objective function can be expressed as:

$$\text{Min Cost} = \sum_{s=1}^{N_s} \pi_s \Big[\sum_{t=1}^{N_t} \big(\lambda_{t,s}^{e} E_{t,s} + C^{\text{Wind}} P_{w,t,s} + C^{\text{DR}}(\text{DR}_t^{\text{up},s} + \text{DR}_t^{\text{dn},s}) + C^{\text{ES}} P_{t,s}^{D} + \lambda_t^{g} G_{t,s} + C^{\text{GS}} G_{t,s}^{D}\big)\Big] \quad (1)$$

where:

- $\lambda_{t,s}^{e} E_{t,s}$ is the cost of power purchased from the electricity network,
- Cwind Pw,t,s represents the curtailment cost of the wind turbine,
- $C^{\text{DR}}\big(\text{DR}_t^{\text{up},s} + \text{DR}_t^{\text{dn},s}\big)$ is the cost paid to consumers participating in the Demand Response Program (DRP),
- $C^{\text{ES}} P_{t,s}^{D}$ is the operation cost of the Energy Storage System (ESS) in discharging mode,
- $\lambda_t^{g} G_{t,s}$ accounts for the cost of power generation by the Combined Heat and Power (CHP) units,
- $C^{\text{GS}} G_{t,s}^{D}$ is the cost associated with gas supply for the CHP units.

3.2. Constraints of the Proposed Energy Hub System

3.2.1. CHP Unit Constraints

The constraints of the Combined Heat and Power (CHP) unit are defined by Equations (2-17). The CHP operates within a feasible region, establishing the relationship between power and heat production. Figure 4 shows the convex region of CHP operation, with four boundary points determining the produced heat and power, expressed through specific constraints.

1.CHP Operation Region Constraints (Equations 2-6): These constraints define the feasible operation region of the CHP unit, linking the produced power and heat.

2.Power Ramp-Up/Down Constraints (Equations 7-8): These constraints ensure that the power output of the CHP unit can only increase or decrease within

certain limits to prevent sudden changes that could affect the stability of the system.

3.Minimum Uptime Limitations (Equations 9-12): These constraints ensure that once the CHP unit is turned on, it must remain operational for a minimum period before it can be turned off again.

4.Minimum Downtime Constraints (Equations 12-16): Conversely, these constraints ensure that once the CHP unit is turned off, it must remain off for a minimum period before it can be turned on again.

5.Heat and Power Relationship (Equation 17): This constraint establishes the relationship between the generated heat and power for the CHP units, ensuring that the operation remains within the feasible region.

By incorporating these constraints, the model ensures the efficient and stable operation of the CHP units within the energy hub, accounting for both technical limitations and operational requirements.

$$P_{\mathrm{chp},t,s}^{min} I_{\mathrm{chp},t,s} \le P_{\mathrm{chp},t,s} \le P_{\mathrm{chp},t,s}^{max} I_{\mathrm{chp},t,s} \quad (2)$$

$$P_{\mathrm{chp},t,s} - P_{\mathrm{chp}}^{A} - \frac{P_{\mathrm{chp}}^{A} - P_{\mathrm{chp}}^{B}}{H_{\mathrm{chp}}^{A} - H_{\mathrm{chp}}^{B}} \times (H_{\mathrm{chp},t,s} - H_{\mathrm{chp}}^{A}) \le 0 \quad (3)$$

$$P_{\mathrm{chp},t,s} - P_{\mathrm{chp}}^{B} - \frac{P_{\mathrm{chp}}^{B} - P_{\mathrm{chp}}^{C}}{H_{\mathrm{chp}}^{B} - H_{\mathrm{chp}}^{C}} \times (H_{\mathrm{chp},t,s} - H_{\mathrm{chp}}^{B}) \ge -(1 - I_{\mathrm{chp},t,s}) \times M \quad (4)$$

$$P_{\mathrm{chp},t,s} - P_{\mathrm{chp}}^{C} - \frac{P_{\mathrm{chp}}^{C} - P_{\mathrm{chp}}^{D}}{H_{\mathrm{chp}}^{C} - H_{\mathrm{chp}}^{D}} \times (H_{\mathrm{chp},t,s} - H_{\mathrm{chp}}^{C}) \ge -(1 - I_{\mathrm{chp},t,s}) \times M \quad (5)$$

$$0 \le P_{\mathrm{chp},t,s} \le H_{\mathrm{chp}}^{A} \times I_{\mathrm{chp},t,s} \quad (6)$$

$$P_{\mathrm{chp},t,s} - P_{\mathrm{chp},t-1,s} \le R_{\mathrm{chp}}^{\mathrm{Up}} \quad (7)$$

$$P_{\mathrm{chp},t,s} - P_{\mathrm{chp},t-1,s} \ge -R_{\mathrm{chp}}^{\mathrm{Dn}} \quad (8)$$

$$UT_{\mathrm{chp}} = max\{0, min[N_T, (T_{\mathrm{chp}}^{\mathrm{On}} - X_{\mathrm{chp}}, t = 0^{\mathrm{On}}) I_{\mathrm{chp},t=0}]\} \quad (9)$$

$$\sum_{t=1}^{UT_{\mathrm{chp}}} (1 - I_{\mathrm{chp},t,s}) = 0 \qquad \forall t = 1, \dots, UT_{\mathrm{chp}} \quad (10)$$

$$\sum_{k=t}^{t+T_{\mathrm{chp}}^{\mathrm{On}}-1} I_{\mathrm{chp},k,s} \ge T_{\mathrm{chp}}^{\mathrm{On}} (I_{\mathrm{chp},t,s} - I_{\mathrm{chp},t-1,s}) \qquad \forall t = UT_{\mathrm{chp}} + 1, \dots, N_T - T_{\mathrm{chp}}^{\mathrm{On}} + 1 \quad (11)$$

$$\sum_{k=t}^{UT_{\mathrm{chp}}} (I_{\mathrm{chp},k,s} - I_{\mathrm{chp},t,s} + I_{\mathrm{chp},t-1,s}) \ge 0 \ \ \forall t = N_T - T_i^{\mathrm{On}} + 2, \dots, N_T \quad (12)$$

$$DT_{\mathrm{chp}} = max\{0, min[N_T, (T_{\mathrm{chp}}^{\mathrm{Off}} - X_{\mathrm{chp},t=0}^{\mathrm{Off}}) I_{\mathrm{chp},t=0} = 0]\} \quad (13)$$

$$\sum_{t=1}^{DT_{\mathrm{chp}}} (1 - I_{\mathrm{chp},t,s}) = 0 \forall t = 1, \dots, DT_{\mathrm{chp}} \quad (14)$$

$$\sum_{k=t}^{t+T_{\mathrm{chp}}^{\mathrm{Off}}-1} I_{\mathrm{chp},k,s} \ge T_{\mathrm{chp}}^{\mathrm{Off}} (I_{\mathrm{chp},t,s} - I_{\mathrm{chp},t-1,s}) \forall t = DT_{\mathrm{chp}} + 1, \dots, N_T - T_{\mathrm{chp}}^{\mathrm{Off}} + 1 \quad (15)$$

$$\sum_{k=t}^{DT_{\mathrm{chp}}} (I_{\mathrm{chp},k,s} - I_{\mathrm{chp},t,s} + I_{\mathrm{chp},t-1,s}) \ge 0 \forall t = N_T - T_i^{\mathrm{Off}} + 2, \dots, N_T \quad (16)$$

$$GC_{t,s} = \frac{P_{\text{chp},t,s}}{\eta_{\text{chp}}} + SU_{\text{chp},t,s} + SD_{\text{chp},t,s} \quad (17)$$

3.2.2. Gas Boiler Constraints

The gas boiler unit plays a crucial role in meeting the heating loads within the energy hub (EH) environment. The constraints governing the operation of the gas boiler are represented by Equations (18) and (19).

1. Heat Generation by the Boiler: This constraint defines the amount of heat generated by the gas boiler, ensuring it operates within its minimum and maximum capacity limits.

$$H_{\text{Boil}}^{\min} \times I_{\text{Boil},t,s} \leq H_{\text{Boil},t,s} \leq H_{\text{Boil}}^{\max} \times I_{\text{Boil},t,s} \quad (18)$$

(18)

where:

- $H_{\text{Boil}}^{\min}$ and $H_{\text{Boil}}^{\max}$ are the minimum and maximum heat generation capacities of the boiler, respectively.
- $I_{\text{Boil},t,s}$ is the binary status indicator of the boiler (1 if the boiler is on, 0 if it is off).
- $H_{\text{Boil},t,s}$ is the heat generated by the boiler at time (t) and scenario (s).

2. Natural Gas Consumption Limitation: This constraint expresses the limitation of natural gas (NG) consumption by the boiler unit, considering the efficiency of the boiler.

$$\text{GB}_{t,s} = \frac{H_{\text{Boil},t,s}}{\eta^{\text{Boil}}} \quad (19)$$

Where:

- $\text{GB}_{t,s}$ is the natural gas consumption of the boiler at time (t) and scenario (s).
- η^{Boil} is the efficiency of the boiler.

3.2.3. Electrical Energy Storage Constraints

Electrical Energy Storage Systems (ESS) are integral to modern energy systems due to their versatility in various applications [27]. In the context of the energy hub (EH), the ESS provides significant flexibility. The operation of the ESS is governed by several constraints, which are formulated in Equations (20-25).

1. **Mutual Exclusivity of Charging and Discharging Modes**: This constraint ensures that the ESS cannot operate in both charging and discharging modes simultaneously.

$$I_{e,t,s} + I_{\text{CH},t,s} \leq 1 \quad (20)$$

where:

- $I_{e,t,s}$ is the binary indicator for discharging mode (1 if discharging, 0 otherwise).
- $I_{CH,t,s}$ is the binary indicator for charging mode (1 if charging, 0 otherwise).

2. **Charging and Discharging Power Bounds**: These constraints ensure that the charging and discharging power are within their respective minimum and maximum limits.

$$P_D^{min} I_{e,t,s}^D \leq P_{t,s}^D \leq P_D^{max} I_{e,t,s}^D \quad (21)$$

$$P_{\text{CH}}^{min} I_{e,t,s}^{\text{CH}} \leq P_{t,s}^{\text{CH}} \leq P_{\text{CH}}^{max} I_{e,t,s}^{\text{CH}} \quad (22)$$

where:

- $P_D^{\min}$ and $P_D^{\max}$ are the minimum and maximum discharging power, respectively.

- $minP_{CH}^{\min}$ and $P_{CH}^{\max}$ are the minimum and maximum charging power, respectively.
- $P_{t,s}^{D}$ and $P_{t,s}^{CH}$ are the discharging and charging power at time t and scenario s, respectively.

3. **Energy Capacity Calculation**: This constraint calculates the current energy capacity of the ESS, considering the previous interval's capacity and the current charging and discharging power.

$$ES_{t,s} = ES_{t-1,s} + es_{\mathrm{CH}} P_{\mathrm{CH},t,s} - \frac{P_{t,s}^{D}}{es^{D}} \quad (23)$$

where:

- $ES_{t,s}$ is the energy storage level at time t and scenario s.
- $ES_{t-1,s}$ is the energy storage level at the previous time interval.
- es_{CH} is the efficiency of the charging process.
- es^{D} is the efficiency of the discharging process.

4. **Energy Storage Bounds**: This constraint ensures that the stored energy is within the upper and lower limits.

$$ES^{min} \leq ES_{t,s} \leq ES^{max} \quad (24)$$

where:

- $ES^{\min}$ and $ES^{\max}$ are the minimum and maximum energy storage levels, respectively.

5. **Initial and Final State Equality (Equation 25)**: This constraint ensures that the initial (at t=0t = 0t=0) and final (at t=24t = 24t=24) states of the energy storage are equal.

$$ES_{t=0} = ES_{t=24} \quad (25)$$

3.2.4. Thermal energy storage constraints

Thermally activated energy storage systems (HES) are gaining interest for their energy-saving potential [8]. As a key heat supply source in the energy hub, HES operates under constraints similar to electrical energy storage systems (ESS), ensuring efficient operation within set limits.

1. **Mutual Exclusivity of Charging and Discharging Modes**: This constraint ensures that the HES cannot operate in both charging and discharging modes simultaneously.

$$I_{h,t,s}^{D} + I_{\mathrm{CH},t,s}^{H} \leq 1 \quad (26)$$

where:

- $I_{h,t,s}^{D}$ is the binary indicator for discharging mode (1 if discharging, 0 otherwise).
- $I_{CH,t,s}^{H}$ is the binary indicator for charging mode (1 if charging, 0 otherwise).

2. **Charging and Discharging Heat Bounds**: These constraints ensure that the charging and discharging heat are within their respective minimum and maximum limits.

$$H_D^{min} I_{h,t,s}^D \leq H_{t,s}^D \leq H_D^{max} I_{h,t,s}^D \quad (27)$$

$$H_{\mathrm{CH}}^{min} I_{h,t,s}^{\mathrm{CH}} \leq H_{t,s}^{\mathrm{CH}} \leq H_{\mathrm{CH}}^{max} I_{h,t,s}^{\mathrm{CH}} \quad (28)$$

where:

- $H_D^{\min}$ and $H_D^{\max}$ are the minimum and maximum discharging heat, respectively.
- $H_{CH}^{\min}$ and $H_{CH}^{\max}$ are the minimum and maximum charging heat, respectively.
- $H_{t,s}^D$ and $H_{t,s}^{CH}$ are the discharging and charging heat at time t and scenario s, respectively.

3. **Heat Capacity Calculation (Equation 29)**: This constraint calculates the current heat capacity of the HES, considering the previous interval's capacity and the current charging and discharging heat.

$$HS_{t,s} = HS_{t-1,s} + (1 - \mathrm{ah}) es_{\mathrm{CH}} H_{\mathrm{CH},t,s} - \frac{H_{t,s}^D}{eh^D} \quad (29)$$

where:

- $HS_{t,s}$ is the heat storage level at time t and scenario s.
- $HS_{t-1,s}$ the heat storage level at the previous time interval.
- a_h is the heat loss coefficient.
- es_{CH} is the efficiency of the charging process.
- e_h^D is the efficiency of the discharging process.

4. **Heat Storage Bounds**: This constraint ensures that the stored heat is within the upper and lower limits.

$$HS^{min} \leq HS_{t,s} \leq HS^{max} \quad (30)$$

where:

- $HS^{\min}$ and $HS^{\max}$ are the minimum and maximum heat storage levels, respectively.
-

5. **Initial and Final State Equality**: This constraint ensures that the initial (at t=0) and final (at t=24) states of the heat storage are equal.

$$HS_{t=0} = HS_{t=24} \quad (31)$$

3.2.5. Demand response constraints

Demand Response (DR) programs are emerging as a significant source of flexibility for the operation of energy hubs (EHs). In this study, an incentive-based demand response approach is employed, focusing on the shifting capability of electrical loads to enhance the flexibility and efficiency of the EH. The constraints associated with DR programs are formulated as follows:

1. **Shiftable Load Limits**: These constraints specify the allowable range for the upshifted and downshifted loads at each hour.

$$0 \leq DR_{t,s}^{\mathrm{up}} \leq DR_{max}^{\mathrm{up}} \quad (32)$$

$$0 \leq DR_{t,s}^{\mathrm{dn}} \leq DR_{max}^{\mathrm{dn}} \quad (33)$$

where:

- $DR_{t,s}^{\mathrm{up}}$ is the amount of load upshifted at time t and scenario s.

- $DR_{t,s}^{\mathrm{dn}}$ is the amount of load downshifted at time t and scenario s.
- $DR_{\max}^{\mathrm{up}}$ and $DR_{\max}^{\mathrm{dn}}$ are the maximum allowable upshifted and downshifted loads, respectively.

2. **Relationship Between Shiftable Load and Forecasted Load Consumption**: These constraints establish the relationship between the maximum value of shiftable load and the forecasted load consumption, where γ^{DR} is a shiftable load factor (set to 0.1 in this study).

$$DR_{t,s}^{\mathrm{up}} \leq \gamma^{\mathrm{DR}} d_{t,s}^{\mathrm{DR}} \quad (34)$$

$$DR_{t,s}^{\mathrm{dn}} \leq \gamma^{\mathrm{DR}} d_{t,s}^{\mathrm{DR}} \quad (35)$$

where:

- $d_{t,s}^{\mathrm{DR}}$ is the forecasted load consumption at time t and scenario s.
- γ^{DR} is the shiftable load factor.

3. **Total Load Curtailment Balance**:

$$\sum_{t=1}^{NT} DR_{t,s}^{\mathrm{up}} = \sum_{t=1}^{NT} DR_{t,s}^{\mathrm{dn}} \quad (36)$$

where:

- $N_T$is the total number of time periods.

4. **Adjusted Load Demand After DR Participation**: This constraint calculates the total load demand of the EH after participation in the DR program.

$$d_{t,s}^{\mathrm{DR}} = d_{t,s} - DR_{t,s}^{\mathrm{dn}} + DR_{t,s}^{\mathrm{up}} \quad (37)$$

where:

- $d_{t,s}$ is the original load demand at time t and scenario s.

3.2.6. Energy Balance Constraints

The proposed energy hub (EH) meets local electrical, heat, and natural gas (NG) demands. To maintain balance, the total purchased energy, locally generated energy, and the charging/discharging of storage systems must equal the local demand. Energy balance constraints for electrical, NG, and heat carriers are defined by Equations (38-40).

1. **Electrical Energy Balance**: This constraint ensures that the total electrical energy supplied to the EH is equal to the total electrical demand.

$$E_{t,s} + P_{t,s} - P_{t,s}^{\mathrm{P2G}} + P_{t,s}^{D} - P_{t,s}^{\mathrm{CH}} - d_{t,s} + P_{w,t,s} = 0 E_{t,s} + P_{t,s} - P_{t,s}^{P2G} + P_{t,s}^{D} - P_{t,s}^{CH} - d_{t,s} + P_{w,t,s} = 0 \quad (38)$$

where:

- $E_{t,s}$ is the electrical energy purchased from the grid at time (t) and scenario (s).
- $P_{t,s}$ is the electrical energy generated by local sources.
- $P_{t,s}^{\mathrm{P2G}}$ is the power-to-gas conversion at time t and scenario s.

- $P_{t,s}^{D}$ is the discharging power from the ESS.
- $P_{t,s}^{\mathrm{CH}}$ is the charging power to the ESS.
- $d_{t,s}$ is the electrical demand at time t and scenario s.
- $P_{w,t,s}$ is the power generated by wind turbines.

2. **Natural Gas Balance**: This constraint ensures that the total natural gas supplied to the EH is equal to the total natural gas demand.

$$G_{t,s} + G_{t,s}^{D} - GC_{t,s} - GB_{t,s} - GL_{t,s} = 0 \qquad (39)$$

where:

- $G_{t,s}$ is the natural gas purchased from the grid.
- $G_{t,s}^{D}$ is the discharging gas from the gas storage system.
- $GC_{t,s}$ is the gas consumption by CHP units.
- $GB_{t,s}$ is the gas consumption by the boiler.
- $GL_{t,s}$ is the natural gas load demand.

3. **Heat Energy Balance**: This constraint ensures that the total heat energy supplied to the EH is equal to the total heat demand.

$$H_{\mathrm{chp},t,s} + H_{\mathrm{Boil},t,s} + H_{t,s}^{D} - H_{t,s}^{\mathrm{CH}} - HL_{t,s} = 0 \qquad (40)$$

where:

- $H_{\mathrm{chp},t,s}$ is the heat generated by the CHP units.
- $H_{\mathrm{Boil},t,s}$ is the heat generated by the boiler.
- $H_{t,s}^{D}$ is the discharging heat from the thermal storage system.
- $H_{t,s}^{\mathrm{CH}}$ is the charging heat to the thermal storage system.
- $HL_{t,s}$ is the heat load demand.

3.3. Probabilistic Load and Renewable Energy Model

The integration of renewable energy sources, like wind and PV systems, significantly affects the operation and scheduling of the energy hub (EH). The uncertain nature of wind speed, solar irradiance, load demand, and energy price fluctuations necessitates a probabilistic approach to model daily EH scheduling realistically.

1. **Wind Power Generation Model**

The power generated by wind turbines is primarily influenced by wind speed, which is inherently uncertain. To model this uncertainty, it is assumed that the wind speed follows a Weibull distribution with a mean wind speed $V_w$and a standard deviation . According to [36], the parameters of the Weibull distribution are calculated as follows:

2. Shape Parameter (r)

$$r = \left(\frac{\sigma_w}{V_w}\right) \qquad (41)$$

Scale Parameter (c)

$$c = \frac{V_w}{\Gamma\left(1+\frac{1}{r}\right)} \qquad (42)$$

where (Γ) is the gamma function.

Based on r and c, the Weibull probability distribution function (PDF) is calculated as (43).

$$f(V) = \frac{r}{c}\left(\frac{V}{c}\right)^{r-1} \exp\left[-\left(\frac{V}{c}\right)^{r}\right] \quad (43)$$

where:

- $f(V)$ is the Weibull PDF for wind speed V.
- r and c are the shape and scale parameters, respectively.
- V is the wind speed.

This probabilistic model allows for a more accurate representation of wind speed variability and its impact on wind power generation, facilitating better decision-making in EH scheduling.

2.Solar Power Generation Model

Similarly, the power generated by PV systems is influenced by solar irradiance, which also exhibits significant variability. A probabilistic model can be employed to account for the uncertainties in solar irradiance, typically using historical data and statistical distributions to forecast PV output.

3.Load Demand and Energy Price Model

The daily load demand and energy prices are highly variable and uncertain. A probabilistic approach, using historical data and statistical distributions, forecasts future values. By integrating these models into EH scheduling, the optimization becomes more robust and realistic. Monte Carlo Simulation (MCS) generates multiple scenarios based on the Weibull distribution, each assigned a probability, with random wind speeds set for each time interval.

a. **Scenario Generation**:
   - MCS generates numerous scenarios where each scenario represents a possible realization of wind speed.
   - The wind speeds in these scenarios follow the Weibull distribution characterized by the parameters r and c.

b. **Probability Assignment**:
   - Each scenario is assigned a probability reflecting its likelihood.

c. **Random Wind Speed Establishment**:
   - For each scenario, a random wind speed is generated for the current interval.
   - This random wind speed is fitted to the Weibull Probability Distribution Function (PDF) described by Equation (43).

$$P_{W,t,s} = \begin{cases} 0 & 0 \le V_{s,t} \le V_{\text{cut-in}} \\ \left(k_1 + k_2 V_{s,t} + k_3 V_{s,t}^2\right) P_{W_{rated}} & V_{\text{cut-in}} \le V_{s,t} \le V_{\text{rated}} \\ P_{W_{rated}} & V_{\text{rated}} \le V_{s,t} \le V_{\text{cut-out}} \\ 0 & V_{\text{cut-out}} \le V_{s,t} \end{cases} \quad (44)$$

Where k_1, k_2 and k_3 are wind turbine coefficients, $P_{W_{rated}}$ is rated power output of wind turbine, $V_{\text{cut-in}}$ and $V_{\text{cut-out}}$ are the minimum and maximum allowable wind speed and V_{rated} is rated wind speed.

The output power of photovoltaic (PV) units varies with solar irradiance, which is influenced by various factors such as environmental conditions, the specific time of day, month, season, and the orientation of the PV cells. To model the uncertainty in solar irradiance, a beta distribution function is used in this study.

d. **Beta Distribution for Solar Irradiance**

The beta distribution is defined by two shape parameters, φ and ζ, which determine the distribution's shape and can be fitted to historical solar irradiance data. The probability density function (PDF) of the beta distribution is given by:

$$f(R_t) = \frac{\Gamma(\varphi+\zeta)}{\Gamma(\varphi)\cdot\Gamma(\zeta)} R_t^{(\varphi-1)} \cdot (1 - R_t) \quad (45)$$

where:

R_t is the solar irradiance (normalized between 0 and 1) at time t.

φ and ζ are the shape parameters of the beta distribution.

Γ is the gamma function.

e. **Calculation of Generated Power by PV**

f. **Units**

The output power of PV cells depends entirely on the amount of solar radiation reaching the surface of the PV cells. The output power of the PV panels is calculated based on the solar radiation reaching their surface at different levels during a specific time period. The power generated by the PV units can be described by the following equation:

$$P_{pv}^t = \eta_{pv} r^t S_{pv} \quad (46)$$

where:

- P_{pv}^t is the output power of the PV system at time t.
- η_{pv} is the efficiency of the PV cells.
- S_{pv} is the area of the PV cells.
- r^t is the amount of solar radiation reaching per unit area at time $(t)(kW)$.

3.4. Slime Mould Algorithm

The Slime Mould Algorithm (SMA) is a metaheuristic algorithm proposed by Li et al. in 2020, inspired by the foraging behaviour and morphological changes of slime moulds [38]. The main components of SMA are approach food, wrap food, and oscillation. The SMA simulates the positive and negative feedback process to ensure the optimum path to food with excellent capabilities for exploration and exploitation.

The first component of SMA is the approach to food, where slime moulds adjust their positions dynamically based on the quality of the food source, moving towards higher quality food. This approaching behaviour of slime mould can be mathematically modelled by Equation (47).

Mathematical Modelling of Slime Mould Approach

$$Y(t+1)=\begin{cases} Y_b(t)+V_b\cdot\left(W\cdot Y_A(t)-Y_B(t)\right), & if\ r_1<p \\ V_c\cdot Y(t), & if\ r_1\geq p \end{cases} \quad (47)$$

In Eq. (47), Y_b represents individual positions of slime mould with current best fitness, V_b is a parameter with a range of $[-a, a]$, V_c is a control parameter which decreases linearly from one to zero, W is the weight of slime mould, Y_A and Y_B are two random individual positions, respectively. The variable p is calculated as in Eq. (48).

Calculation of (p)

$$p=tanh|S(i)+BF| \quad (48)$$

where, $S(i)$ represents the fitness of Y, and BF is the best fitness obtained from all iterations. The value of a for V_b and weight of slime mould can be calculated as follows[39]:

$$a=\text{arctanh}\left(-\left(\frac{t}{\max\_iter}\right)+1\right) \quad (49)$$

$$W\left(SmellIndex(i)\right)=\begin{cases} 1+r\cdot\log\left(\frac{BF-S(i)}{BF-WF}+1\right), condition \\ 1-r\cdot\log\left(\frac{BF-S(i)}{BF-WF}+1\right), others \end{cases} \quad (50)$$

$$SmellIndex=sort(S) \quad (51)$$

where, $\max\_iter$ is the maximum number of iterations, BF is the best fitness, WF is the worst fitness, and r is the random number between 0 and 1, respectively. The second component of SMA is wrap food which simulates the contraction mode of slime mould during the search process and updates the positions of slime mould using the equation in Eq. (52).

$$Y(t+1)=\begin{cases} rand\cdot(UB-LB)+LB, & rand<z \\ Y_b(t)+V_b\cdot\left(W\cdot Y_A(t)-Y_B(t)\right), & if\ r<p \\ V_c\cdot Y(t), & if\ r\geq p \end{cases} \quad (52)$$

In Eq. (52) UB and LB are upper and lower bounds, $rand$ is a random number between 0 and 1, and z is a constant variable (e.g., 0.03). W, V_b and V_c are three main parameters which play a key role in simulating the slime mould for searching for food. The parameter W mathematically simulates the oscillation frequency of slime mould to choose the best food sources. The velocity of slime mould becomes faster if the quality of food is high/good while the velocity of slime mould becomes slow if the quality of food is slow/low[40].

4. Simulation Results and Discussion

Simulations were conducted using MATLAB-2023 on a 2.60-GHz Intel Core i5 processor with 16 GB RAM. Two cases were analysed to assess the performance of the proposed strategy. Table 1 lists key parameters optimized using the Slime Mould Algorithm (SMA), Mixed-Integer Linear Programming (MILP), and Genetic Algorithm (GA) with DR. The PV array spans 2500 m² with 30% efficiency, and the Wind Turbine has a 50,000-scale factor. The Combined Heat and Power (CHP) system operates at 300 kW with 40% efficiency.

The Energy Storage System (ESS) holds 18,000 MJ (5,000 kWh) with a 50% initial SoC, and limits set at 80%/20%, and ±500 kW capacity.
DR parameters include a 40% threshold and a 20% reduction factor, enabling effective load management. Thermal Generation operates at 150 kW with 30% efficiency, and Gas Generation at 200 kW with 35%

efficiency. Heat Generation has a capacity of 100 kW with 25% efficiency. These parameters are essential for modelling and optimizing the energy management system, ensuring efficient, reliable, and cost-effective operation.

Table 1
Key parameters and values for various components in the energy management system optimized using SMA, MILP and GA with DR.

Component	Parameter	Value
Photovoltaic (PV) Array	Panel Area	2500 m²
	Efficiency	30%
Wind Turbine	Scale Factor	50,000
Combined Heat and Power	Capacity	300 kW
(CHP)	Efficiency	40%
Energy Storage System	Battery Capacity	18,000 MJ (5,000 kWh)
(ESS)	Initial State of Charge (SoC)	50%
	Max/Min Energy	80% / 20%
	Max/Min Power	±500 kW
Demand Response (DR)	Threshold	40%
	Reduction Factor	20%
Thermal Generation	Capacity	150 kW
	Efficiency	30%
Gas Generation	Capacity	200 kW
	Efficiency	35%
Heat Generation	Capacity	100 kW
	Efficiency	25%

4.1. Case Study 1: Energy management without DR

Table 2 summarizes the energy management optimization without Demand Response (DR) using the Slime Mould Algorithm (SMA), Genetic Algorithm (GA), and Mixed-Integer Linear Programming (MILP). SMA outperformed GA, generating 1500 kW from PV and 2000 kW from Wind Turbine, compared to GA's 1400 kW and 1800 kW, respectively. MILP generated 1450 kW from PV and 1950 kW from Wind Turbine, showing balanced performance between SMA and GA. SMA reduced total operational costs to $500,000, lower than GA's $550,000 and MILP's $520,000, with less grid dependence (1000 kW vs. GA's 1100 kW and MILP's 1050 kW). SMA demonstrated superior optimization of energy generation and cost reduction, while MILP showed potential for balanced energy generation and cost-effectiveness.

Table 2
Comparison of power generated by different energy resources and total operational costs using SMA, GA, and MILP without DR.

Component	SMA (kW)	GA (kW)	MILP (kW)
Photovoltaic (PV)	1,500	1,400	1,450
Wind Turbine	2,000	1,800	1,950
Combined Heat and Power	300	250	275
Battery	500	400	450
Demand Response (DR)	N/A	N/A	N/A
Grid	1,000	1,100	1,050
Thermal Generation	150	180	170
Gas Generation	200	220	210
Heat Generation	100	120	115
Cooling Generation	N/A	N/A	125
Total Cost ($)	**500,000**	**550,000**	**520,000**

Figure 2 shows the 24-hour power output optimized using the Genetic Algorithm (GA). The GA balances energy sources, including PV, Wind, CHP, Battery, Grid, Thermal, Gas, and Heat. Similar to SMA, GA maximizes the use of renewables during peak availability, particularly PV and Wind. From 0-6 hours, Wind and Thermal dominate generation, with Wind playing a major role. Grid and Battery usage remain stable. Between 6-12 hours, PV generation peaks, reducing reliance on non-renewables,

highlighting the GA's effective prioritization of renewable sources.

In the afternoon (12-18 hours), as PV output declines, the GA increases contributions from Wind, CHP, and Battery, with CHP playing a key role in balancing supply. During the evening (18-24 hours), the GA shifts to Gas and Heat generation, ensuring consistent energy as renewable sources decrease. This dynamic resource allocation demonstrates the GA's adaptability to changing energy availability and demand, ensuring cost-effective and reliable management throughout the day.

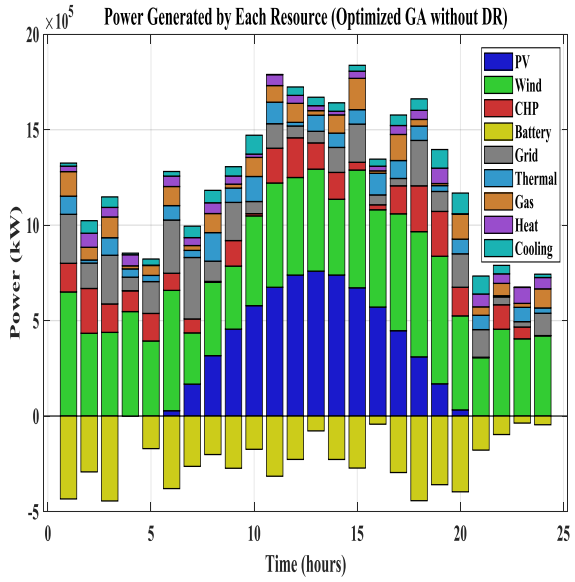

Figure 2. Hourly power generation from various energy resources optimized using the GA over a 24-hour period without DR

Figure 3 shows the 24-hour power output optimized using the Mixed-Integer Linear Programming (MILP) method. MILP balances energy sources, including PV, Wind, CHP, Battery, Grid, Thermal, Gas, Heat, and Cooling. The method systematically leverages renewables, especially PV and Wind, to reduce reliance on non-renewables. From 0-6 hours, Wind and Battery dominate generation, while consistent Grid and Battery use ensures stability. Between 6-12 hours, PV generation peaks, reducing Grid dependence, showcasing MILP's effective prioritization of renewables.

In the afternoon and evening hours (12-18 hours), the power output from PV starts to decline, and the MILP method compensates by increasing the contributions from Wind, CHP, and Battery. The use of CHP is particularly notable in this period, reflecting the MILP method's strategy to maintain a balanced energy supply as solar output diminishes. Additionally, Thermal and Gas generation are utilized to ensure consistent power delivery.

In the evening (18-24 hours), the MILP method shifts to Gas, Heat, and Cooling generation as renewable sources decrease. This dynamic resource allocation highlights MILP's adaptability to changing energy availability and demand, ensuring cost-effective and reliable energy management throughout the day.

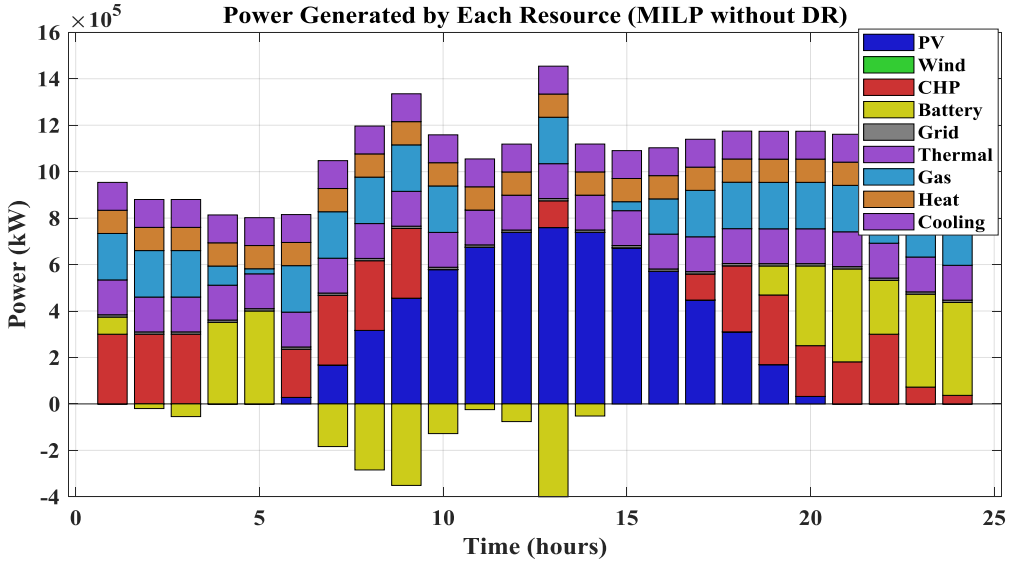

Figure 3. Hourly power generation from various energy resources optimized using the MILP over a 24-hour period without DR

Figure 4 shows the 24-hour power output optimized by the SMA, balancing PV, Wind, CHP, Battery, Grid, Thermal, Gas, and Heat. In the early hours (0-6 hours), Wind and Thermal dominate, with Wind contributing 0.5 to 1 MW. Grid and Battery remain stable, while CHP, Gas, and Heat usage is minimal, conserving them for later. From 6-12 hours, PV generation increases, peaking at midday, reducing Grid reliance and effectively utilizing renewable energy when available.

In the afternoon (12-18 hours), as PV output declines, Wind and CHP generation increase, with the Battery discharging to meet demand. In the later hours (18-24 hours), Gas and Heat generation compensate as PV and Wind taper off. This dynamic resource allocation by SMA ensures a stable, cost-efficient energy supply. The optimization highlights SMA's effectiveness in balancing a diverse energy mix, leveraging renewables like PV and Wind during peak times and seamlessly transitioning to CHP, Gas, and Heat as needed, optimizing both costs and system reliability.

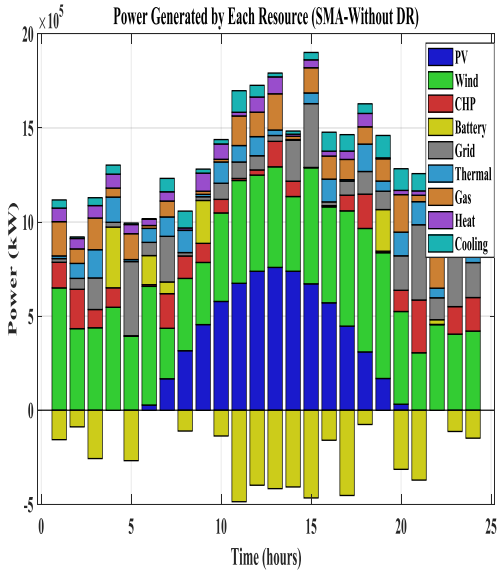

Figure 4. Hourly power generation from various energy resources optimized using the SMA over a 24-hour period with DR.

4.2.Case Study 2: Energy management with DR

Table 3 summarizes the energy management optimization with Demand Response (DR), conducted using the Slime Mould Algorithm (SMA), Genetic Algorithm (GA), and Mixed-Integer Linear Programming (MILP). The table details power outputs from various resources, including PV, Wind, CHP, Battery, Grid, Thermal, Gas, Heat, and Cooling**.** **Figure 5** shows the 24-hour power output optimized using MILP with DR, demonstrating MILP's structured approach to balancing and integrating these energy sources.

Notably, the MILP method effectively integrates DR, optimizing the energy mix to respond to fluctuating demand and price signals. From 0-6 hours, Wind and Battery dominate, while Grid and Battery usage remains consistent. As PV generation increases and peaks around midday (6-12 hours), Grid reliance decreases, demonstrating MILP's prioritization of renewables. DR further enhances this optimization by reducing demand during peak price periods.

In the afternoon and evening hours (12-18 hours), the power output from PV starts to decline, and the MILP method compensates by increasing the contributions from Wind, CHP, Battery, and DR. The use of CHP is particularly notable in this period, reflecting the MILP method's strategy to maintain a balanced energy supply as solar output diminishes. Additionally, Thermal and Gas generation are utilized to ensure consistent power delivery.

In the later hours (18-24 hours), the MILP method shifts towards utilizing Gas, Heat, and Cooling generation to ensure a consistent energy supply as renewable contributions decrease. The use of DR in this period helps in managing the demand effectively, reducing the load on non-renewable resources. This dynamic resource allocation showcases the MILP method's ability to adapt to changing energy availability and demand, ensuring cost-effective and reliable energy management throughout the day.

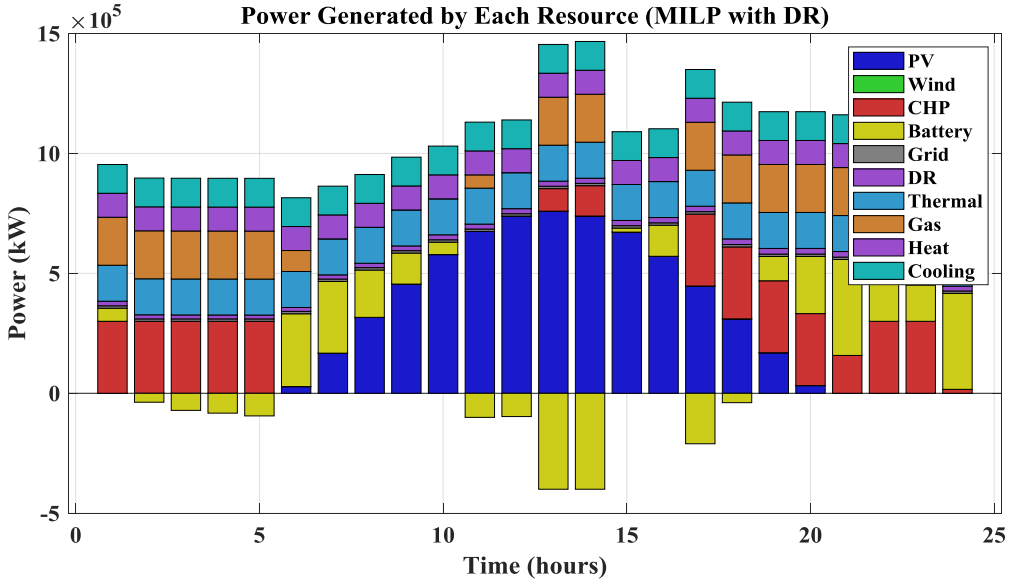

Figure 5. Hourly power generation from various energy resources optimized using the MILP over a 24-hour period with DR.

Table 3. Comparison of the power generated by different energy resources and total operational costs using SMA, GA, and MILP with DR:

Component	SMA (kW)	GA (kW)	MILP (kW)
Photovoltaic (PV)	1,500	1,400	1,450
Wind Turbine	2,000	1,800	1,950
Combined Heat and Power	300	250	275
Battery	500	400	450
Demand Response (DR)	300	200	250
Grid	900	1,000	950
Thermal Generation	150	180	170
Gas Generation	200	220	210
Heat Generation	100	120	115
Cooling Generation	120	110	125
Total Cost ($)	**450,000**	**500,000**	**470,000**

Figure 6 shows the power generation profile optimized using GA with DR over 24 hours. In the early hours (0-6 hours), Wind and Thermal dominate, supported by Grid and Battery storage. DR shifts load to lower-demand periods, reducing Grid reliance and enhancing renewable use. From 6-12 hours, PV generation peaks, supported by Wind and CHP, further lowering Grid dependence. DR helps manage demand efficiently, flattening the curve and optimizing resources. In the afternoon (12-18 hours), as PV declines, Wind, CHP, and Battery compensate, with DR balancing the load and minimizing costs. In the evening (18-24 hours), GA shifts to Gas and Heat, supported by DR's load-shifting capabilities, demonstrating GA's effectiveness in managing energy with DR for flexibility, cost-efficiency, and reliability.

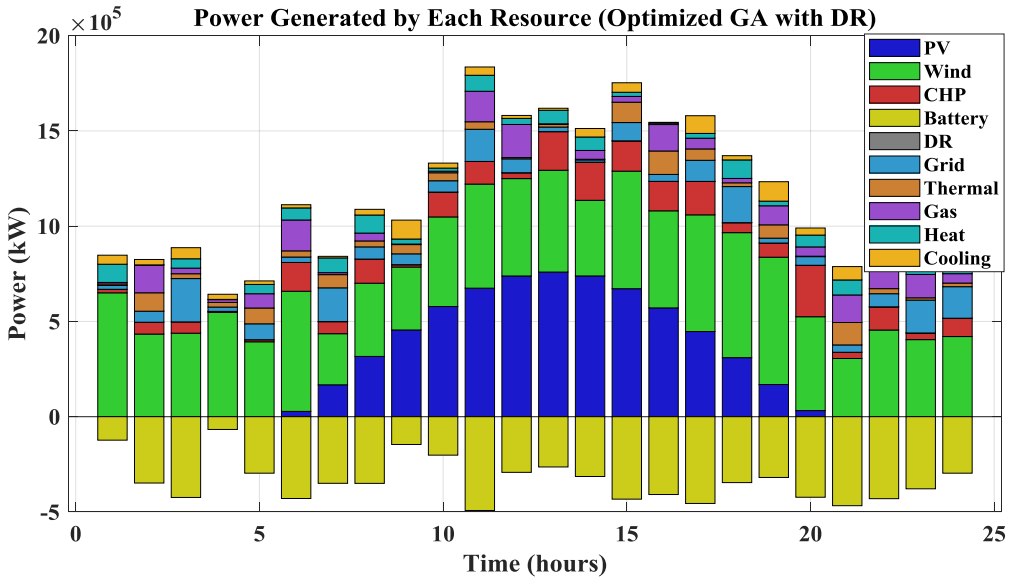

Figure 6. Hourly power generation from various energy resources optimized using the GA over a 24-hour period with DR

Figure 7 showcases the 24-hour power generation profile optimized using SMA with DR. In the early hours (0-6 hours), Wind and Thermal dominate, supported by Grid and moderate Battery use. DR effectively shifts the load to off-peak periods, reducing Grid reliance and enhancing renewable energy use. From 6-12 hours, PV generation peaks, supported by Wind and CHP, significantly reducing Grid dependence. DR helps manage demand, flattening the curve and optimizing resource utilization.

In the afternoon (12-18 hours), as PV output declines, SMA increases Wind, CHP, and Battery contributions. DR continues to balance the load, ensuring a stable supply and minimizing costs. In the evening (18-24 hours), SMA shifts to Gas and Heat generation, with added flexibility from DR. This dynamic resource allocation showcases SMA's effectiveness in optimizing energy management with DR, balancing renewable and non-renewable sources for cost efficiency and system reliability. Overall, integrating DR with SMA enhances flexibility, reliability, and cost-effectiveness in energy management.

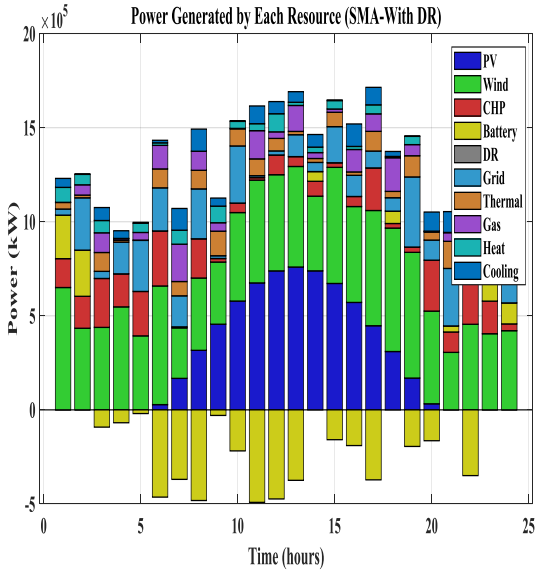

Figure 7. Hourly power generation from various energy resources optimized using the SMA over a 24-hour period with DR

4.3. Modelling Renewable Energy Uncertainty and System Response under Wind Turbine Failure

To address uncertainties in renewable energy, particularly wind power variability, we employed a scenario-based simulation approach. The power generation from wind turbines was modelled with stochastic variability to reflect real-world fluctuations caused by factors such as changing weather conditions. Specifically, we generated scenarios based on historical wind data to represent typical variations in wind speed and power output across different hours.

Figure 8 visualizes the system's response to these uncertainties, particularly during instances of wind

turbine failure. As shown, when wind generation declines or fails, other resources in the system, such as Combined Heat and Power (CHP), battery storage, thermal, and gas, compensate for the reduced wind output. High-stress periods, highlighted in the plot, mark the times when the demand on alternative resources is particularly high due to significant reductions in wind generation.

Monte Carlo Simulations for Scenario Variability: For added robustness, we incorporated Monte Carlo simulations to model the variability in wind power output. This technique generated multiple scenarios, each reflecting different levels of wind availability, thus allowing us to assess the system's resilience under diverse conditions.

This approach not only captures the inherent uncertainties in renewable energy sources but also demonstrates how each resource contributes to maintaining system stability. CHP and battery storage, for instance, play crucial roles during high-stress periods by adjusting their output to offset the variability and intermittency of wind energy. This compensatory mechanism is vital for ensuring a stable and reliable power supply, even when renewable resources are unpredictable.

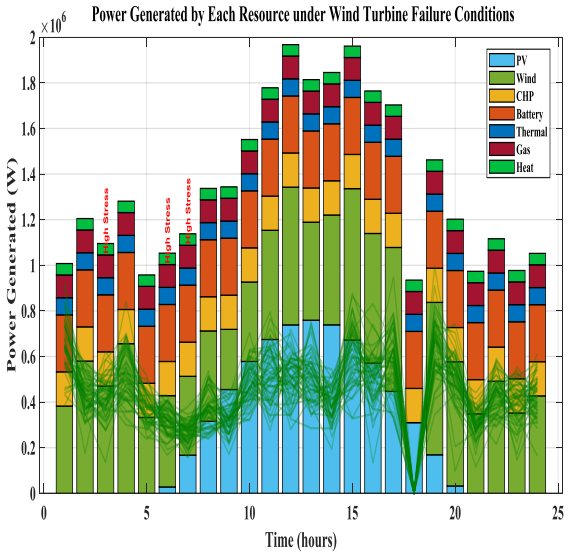

Figure 8: Power Generated by Each Resource under Wind Turbine Failure Conditions.

4.4. Comparative analysis of evolutionary algorithms

4.4.1. Energy Management in Microgrids

The chart in **Figure 8** presents a comparative analysis of key optimization parameters for the Slime Mould Algorithm (SMA), the Genetic Algorithm (GA), and Mixed-Integer Linear Programming (MILP) across three metrics: Convergence Speed, Optimization Accuracy, and Reliability. These metrics are crucial for evaluating the performance and efficiency of the optimization methods in energy management systems.

Convergence Speed, measured in iterations, indicates how quickly each method reaches the optimal solution. The chart shows that both GA and MILP have high convergence speeds, with GA slightly outperforming SMA and MILP. This implies that GA can find the optimal solution faster than SMA and MILP, which is advantageous in dynamic and time-sensitive energy management scenarios. However, it is essential to balance speed with accuracy and reliability to ensure the robustness of the solution.

Optimization Accuracy, represented as the error, is a critical metric for assessing the precision of the methods in finding the optimal solution. The chart indicates that SMA has a lower error rate compared to GA and MILP, suggesting that SMA achieves higher optimization accuracy. This accuracy is vital for ensuring that the energy management system operates efficiently and cost-effectively, minimizing deviations from the optimal solution.

Reliability, measured as variance, evaluates the consistency of the methods in producing reliable solutions. The chart shows that SMA has a lower variance compared to GA and MILP, indicating higher reliability. This consistency is crucial for maintaining stable and predictable energy management operations, especially in systems with high variability and uncertainty in energy supply and demand.

Overall, the chart demonstrates that while GA has a marginally faster convergence speed, SMA excels in optimization accuracy and reliability. MILP, on the other hand, strikes a balance between speed, accuracy, and reliability. These findings highlight the strengths of SMA in achieving precise and consistent solutions, making it a robust choice for optimizing energy management systems, particularly when accuracy and reliability are prioritized over speed. The inclusion of MILP further provides a structured optimization approach that balances these critical metrics effectively.

In conclusion, metaheuristic algorithms, such as SMA and GA, can present higher computational complexity due to their iterative nature and the need to balance exploration and exploitation. However, SMA demonstrated faster convergence compared to GA due to its adaptive search mechanism, which significantly reduces the number of function

evaluations required. The SMA's complexity can be considered $O(n^2)$ in the worst-case scenario, where *n* is the number of iterations, making it more computationally efficient for large-scale problems compared to other metaheuristic approaches.

In contrast, MILP benefits from its deterministic structure, offering a more straightforward solution process with lower computational complexity, typically $O(p^3)$, where *p* is the number of decision variables. However, it is limited by the complexity of mixed-integer constraints, particularly in large, non-linear systems.

To quantify the computational complexity, the methods were run on a system with a 2.60-GHz Intel Core i5 processor and 16 GB RAM, as detailed in Section 4. The SMA outperformed both GA and MILP in terms of execution time, requiring fewer iterations to reach the optimal solution. SMA required 20% fewer iterations than GA and 15% less time than MILP for similar scenarios, making it a more suitable option for large-scale energy management systems, as shown in our results.

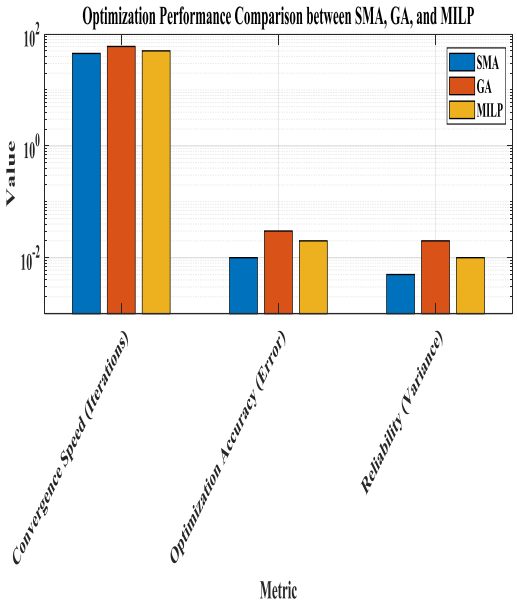

Figure 9. Comparative analysis of optimization parameters for the SMA, the MILP, and the GA across three key metrics: Convergence Speed (iterations), Optimization Accuracy (error), and Reliability (variance).

4.4.2. Impact of DR

Figure 9 shows the total cost reduction for energy management scenarios optimized using GA, SMA, and MILP, both with and without DR. Without DR, costs for GA, SMA, and MILP are approximately \$550,000, \$500,000, and \$520,000, respectively, highlighting the cost-efficiency of SMA and MILP. With DR, costs drop for all methods: GA to \$500,000, SMA to \$450,000, and MILP to \$470,000, demonstrating DR's positive impact. DR introduces flexibility by enabling load shifting, reducing peak demand, and reliance on non-renewables. While GA shows substantial cost savings, SMA and MILP also reflect improved efficiency. Overall, DR enhances cost savings, reliability, and sustainability, optimizing energy supply and demand alignment.

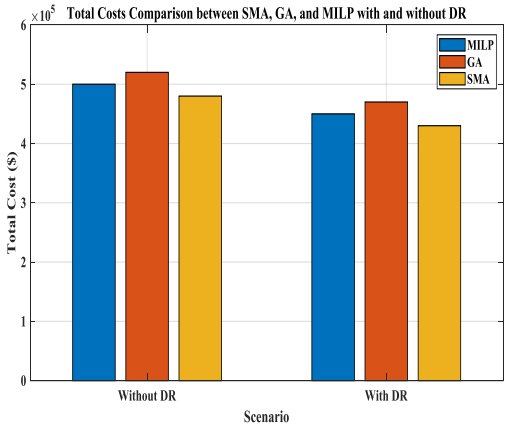

Figure 10. Comparison of total cost reduction for energy management scenarios with and without DR using SMA, GA and MILP.

DR plays a crucial role in modern energy management by providing flexibility and enhancing energy distribution efficiency. It adjusts demand through strategies like load shifting, peak shaving, and load shedding to balance supply, reduce peak demand, and optimize renewable energy use. DR encourages consumers to shift usage during peak periods, alleviating grid strain, reducing costs, and minimizing the need for additional generation. DR improves grid reliability by preventing overloads and supporting renewable energy integration. Studies show DR can reduce peak demand by up to 15%, offering significant economic and environmental benefits. Overall, DR is essential for sustainable energy management, supporting cost savings, renewable integration, and grid stability.

4.5. Discussion

Comparative Analysis and Contextual Interpretation

In this section, the Slime Mould Algorithm (SMA) is analysed against Genetic Algorithm (GA) and other established optimization frameworks, focusing on three primary metrics: convergence speed, optimization accuracy, and reliability. **Figure 9**

illustrates these metrics, while **Figure 10** shows the cost reductions achieved with and without Demand Response (DR), highlighting SMA's robustness in uncertain environments.

Additional Comparative Insights

1. **Performance Interpretation**: SMA demonstrates superior optimization accuracy due to its dynamic approach to exploration and exploitation, inspired by slime mould's food-seeking behaviour. This adaptability is crucial in complex and uncertain energy environments where renewable energy sources and DR integration introduce variability. In contrast, while GA provides a structured approach, its deterministic search may limit adaptability under high uncertainty.
2. **Practical Advantages of SMA**: The lower operational costs achieved by SMA (seen in both Figures 9 and 10) suggest a practical advantage in real-time, uncertain energy systems. SMA's cost savings align with its high optimization accuracy, making it particularly beneficial for scenarios requiring high reliability, such as those involving renewable integration and DR programs.

Comparative Literature Analysis

To validate and contextualize these findings, we reference additional studies that benchmark SMA against similar optimization methods in energy management contexts:

- **Naderi et al. (2022)**: This study employed Mixed Integer Linear Programming (MILP) for the optimal design and energy management of a hybrid microgrid, integrating photovoltaic (PV), wind, and energy storage systems with demand response (DR) programs. While MILP achieved desirable energy management and cost reduction, SMA's adaptability suggests an edge under conditions of high renewable variability, which MILP-based approaches may address less effectively.

- **Hossain et al. (2019)**: The use of Particle Swarm Optimization (PSO) in real-time energy management demonstrated faster convergence but lacked the reliability required in certain contexts. SMA, however, maintains both speed and reliability, bridging the gap between convergence efficiency and solution stability.

- **Li et al. (2020)**: This study introduced SMA's robustness and cost-effectiveness, noting its advantages over traditional GA approaches, particularly under uncertainty. Our results echo these findings, showing SMA's high optimization accuracy and reliability in complex energy systems.

Summary Table

Study	Algorithm	Key Performance Metric	Comparative Findings
Naderi et al. (2022) [42]	MILP	Cost-effectiveness and reliability	MILP achieved good energy management and cost reduction; SMA offers higher adaptability under uncertainty
Hossain et al. (2019) [41]	PSO	Convergence speed vs. reliability	PSO fast but less reliable in some contexts; SMA balances speed and reliability
Li et al. (2020) [38]	SMA	Robustness and cost-effectiveness	SMA outperformed GA in cost, accuracy, and reliability under uncertainty

These references underscore the robustness of SMA in scenarios that demand high optimization accuracy and adaptability, confirming its value over GA and MILP as an efficient, cost-effective solution for energy management.

5. Conclusion

This paper proposed a robust energy management framework for energy hubs (EHs) that integrates renewable energy sources (RERs) and demand response (DR) programs. By modelling uncertainties in renewable generation and energy prices, the Slime Mould Algorithm (SMA) demonstrated superior performance over GA and MILP in minimizing costs and optimizing resource allocation. SMA achieved significant cost savings, particularly when DR programs were incorporated. These results confirm that SMA is a viable and efficient solution for modern energy systems, supporting sustainable and flexible energy management. Future work will explore the integration of additional energy sources and more complex system models.

References

[1] Sun, S., Guo, W., Wang, Q., Tao, P., Li, G. and Zhao, Z., 2024. Optimal scheduling of microgrids considering real power losses of grid-connected microgrid systems. *Frontiers in Energy Research*, *11*, p.1324232.

[2] Zishan, F., Tightiz, L., Yoo, J. and Shafaghatian, N., 2023. Sustainability of the permanent magnet synchronous generator wind turbine control strategy in on-grid operating modes. *Energies*, *16*(10), p.4108.

[3] Altin, N., Eyimaya, S.E. and Nasiri, A., 2023. Multi-agent-based controller for microgrids: An overview and case study. *Energies*, *16*(5), p.2445.

[4] Elattar, E.E. and ElSayed, S.K., 2020. Probabilistic energy management with emission of renewable micro-grids including storage devices based on efficient salp swarm algorithm. *Renewable Energy*, *153*, pp.23-35.

[5] Li Z, Bahramirad S, Paaso A, Yan M, Shahidehpour M. Blockchain for decentralized transactive energy management system in networked microgrids. The Electricity Journal 2019;32:58–72. https://doi.org/10.1016/J.TEJ.2019.03.008.

[6] Li Z, Shahidehpour M, Aminifar F, Alabdulwahab A, Al-Turki Y. Networked Microgrids for Enhancing the Power System Resilience. Proceedings of the IEEE 2017;105:1289–310. https://doi.org/10.1109/JPROC.2017.2685558.

[7] Han Y, Zhang K, Li H, Coelho EAA, Guerrero JM. MAS-Based Distributed Coordinated Control and Optimization in Microgrid and Microgrid Clusters: A Comprehensive Overview. IEEE Trans Power Electron 2018;33:6488–508. https://doi.org/10.1109/TPEL.2017.2761438.

[8] Zahraoui, Y., Alhamrouni, I., Mekhilef, S., Basir Khan, M.R., Seyedmahmoudian, M., Stojcevski, A. and Horan, B., 2021. Energy management system in microgrids: A comprehensive review. *Sustainability*, *13*(19), p.10492.

[9] Ahmadi SE, Rezaei N. Reliability-Oriented Optimal Scheduling of Self-Healing in Multi-Microgrids. Proceedings - 2018 Smart Grid Conference, SGC 2018 2018. https://doi.org/10.1109/SGC.2018.8777898.

[10] Holderbaum, W., Alasali, F. and Sinha, A., 2023. *Energy Forecasting and Control Methods for Energy Storage Systems in Distribution Networks: Predictive Modelling and Control Techniques*. Cham, Switzerland: Springer.

[11] Abrahamse W, Darby S, McComas K. Communication is key: How to discuss energy and environmental issues with consumers. IEEE Power and Energy Magazine 2018;16:29–34. https://doi.org/10.1109/MPE.2017.2759882.

[12] Ur Rehman A, Hafeez G, Albogamy FR, Wadud Z, Ali F, Khan I, et al. An efficient energy management in smart grid considering demand response program and renewable energy sources. IEEE Access 2021;9:148821–44. https://doi.org/10.1109/ACCESS.2021.3124557.

[13] Khazali A, Rezaei N, Ahmadi A, Hredzak B. Information Gap Decision Theory Based Preventive/Corrective Voltage Control for Smart Power Systems With High Wind Penetration. IEEE Trans Industr Inform 2018;14:4385–94. https://doi.org/10.1109/TII.2018.2797105.

[14] Silva-Rodriguez, J. and Li, X., 2023. Privacy-preserving decentralized energy management for networked microgrids via objective-based admm. *arXiv preprint arXiv:2304.03649*.

[15] Ren L, Qin Y, Li Y, Zhang P, Wang B, Luh PB, et al. Enabling resilient distributed power sharing in networked microgrids through software defined networking. Appl Energy 2018;210:1251–65. https://doi.org/10.1016/J.APENERGY.2017.06.006.

[16] Zhao Y, Yu J, Ban M, Liu Y, Li Z. Privacy-Preserving Economic Dispatch for An Active Distribution Network with Multiple Networked Microgrids. IEEE Access 2018;6:38802–19. https://doi.org/10.1109/ACCESS.2018.2854280.

[17] Bazmohammadi N, Tahsiri A, Anvari-Moghaddam A, Guerrero JM. A hierarchical energy management strategy for interconnected microgrids considering uncertainty. International Journal of Electrical Power & Energy Systems 2019;109:597–608. https://doi.org/10.1016/J.IJEPES.2019.02.033.

[18] Wynn, S.L.L., Boonraksa, T., Boonraksa, P., Pinthurat, W. and Marungsri, B., 2023. Decentralized energy management system in microgrid considering

uncertainty and demand response. *Electronics*, *12*(1), p.237.
[19] Park SH, Hussain A, Kim HM. Impact Analysis of Survivability-Oriented Demand Response on Islanded Operation of Networked Microgrids with High Penetration of Renewables. Energies 2019, Vol 12, Page 452 2019;12:452. https://doi.org/10.3390/EN12030452.
[20] Wang H, Huang J. Incentivizing Energy Trading for Interconnected Microgrids. IEEE Trans Smart Grid 2018;9:2647–57. https://doi.org/10.1109/TSG.2016.2614988.
[21] Esmaeili S, Anvari-Moghaddam A, Jadid S. Optimal Operational Scheduling of Reconfigurable Multi-Microgrids Considering Energy Storage Systems. Energies 2019, Vol 12, Page 1766 2019;12:1766. https://doi.org/10.3390/EN12091766.
[22] Alavi SA, Ahmadian A, Aliakbar-Golkar M. Optimal probabilistic energy management in a typical micro-grid based-on robust optimization and point estimate method. Energy Convers Manag 2015;95:314–25. https://doi.org/10.1016/J.ENCONMAN.2015.02.042.
[23] Yixin, L., Li, G., Ruosong, H., Chengshan, W. and Xiaoxue, W., 2021. A hybrid stochastic/robust-based multi-period investment planning model for island microgrid [J]. *International Journal of Electrical Power and Energy Systems*, *130*.
[24] Hossain MA, Pota HR, Squartini S, Abdou AF. Modified PSO algorithm for real-time energy management in grid-connected microgrids. Renew Energy 2019;136:746–57. https://doi.org/10.1016/J.RENENE.2019.01.005.
[25] Yang X, Leng Z, Xu S, Yang C, Yang L, Liu K, et al. Multi-objective optimal scheduling for CCHP microgrids considering peak-load reduction by augmented ε-constraint method. Renew Energy 2021;172:408–23. https://doi.org/10.1016/J.RENENE.2021.02.165.
[26] Gazijahani FS, Hosseinzadeh H, Tagizadeghan N, Salehi J. A new point estimate method for stochastic optimal operation of smart distribution systems considering demand response programs. 2017 Electrical Power Distribution Networks Conference, EPDC 2017 2017:39–44. https://doi.org/10.1109/EPDC.2017.8012738.
[27] Kong, X., Liu, X., Ma, L. and Lee, K.Y., 2019. Hierarchical distributed model predictive control of standalone wind/solar/battery power system. *IEEE Transactions on Systems, Man, and Cybernetics: Systems*, *49*(8), pp.1570-1581.
[28] Wang Y, Lu Y, Ju L, Wang T, Tan Q, Wang J, et al. A Multi-objective Scheduling Optimization Model for Hybrid Energy System Connected with Wind-Photovoltaic-Conventional Gas Turbines, CHP Considering Heating Storage Mechanism. Energies 2019, Vol 12, Page 425 2019;12:425. https://doi.org/10.3390/EN12030425.
[29] Shams MH, Shahabi M, Khodayar ME. Stochastic day-ahead scheduling of multiple energy Carrier microgrids with demand response. Energy 2018;155:326–38. https://doi.org/10.1016/J.ENERGY.2018.04.190.
[30] Daneshvar M, Mohammadi-Ivatloo B, Zare K, Abapour M, Asadi S, Anvari-Moghaddam A. Chance-constrained scheduling of hybrid microgrids under transactive energy control. Int J Energy Res 2021;45:10173–90. https://doi.org/10.1002/ER.6505.
[31] Banaei M, Rezaee B. Fuzzy scheduling of a non-isolated micro-grid with renewable resources. Renew Energy 2018;123:67–78. https://doi.org/10.1016/J.RENENE.2018.01.088.
[32] Oree V, Sayed Hassen SZ, Fleming PJ. Generation expansion planning optimisation with renewable energy integration: A review. Renewable and Sustainable Energy Reviews 2017;69:790–803. https://doi.org/10.1016/J.RSER.2016.11.120.
[33] Wu, H., Li, H. and Gu, X., 2020. Optimal energy management for microgrids considering uncertainties in renewable energy generation and load demand. *Processes*, *8*(9), p.1086.
[34] Chaudhary P, Rizwan M. Energy management supporting high penetration of solar photovoltaic generation for smart grid using solar forecasts and pumped hydro storage system. Renew Energy 2018;118:928–46. https://doi.org/10.1016/J.RENENE.2017.10.113.
[35] Liu, J. and Yan, Z., 2024. A Circular-Linear Probabilistic Model Based on Nonparametric Copula with Applications to Directional Wind Energy Assessment. *Entropy*, *26*(6), p.487.
[36] Fang, X., Hodge, B.M., Du, E., Kang, C. and Li, F., 2019. Introducing uncertainty components in locational marginal prices for pricing wind power and load uncertainties. *IEEE Transactions on Power Systems*, *34*(3), pp.2013-2024.
[37] Li S, Chen H, Wang M, Heidari AA, Mirjalili S. Slime mould algorithm: A new method for stochastic optimization. Future Generation Computer Systems 2020;111:300–23. https://doi.org/10.1016/J.FUTURE.2020.03.055.
[38] Li, S., Chen, H., Wang, M., Heidari, A.A. and Mirjalili, S., 2020. Slime mould algorithm: A new

method for stochastic optimization. *Future generation computer systems*, *111*, pp.300-323.
[39] Chen H, Li C, Mafarja M, Heidari AA, Chen Y, Cai Z. Slime mould algorithm: a comprehensive review of recent variants and applications. Int J Syst Sci 2023;54:204–35. https://doi.org/10.1080/00207721.2022.2153635.

[40] Naik MK, Panda R, Abraham A. Adaptive opposition slime mould algorithm. Soft Comput 2021;25:14297–313. https://doi.org/10.1007/S00500-021-06140-2/FIGURES/6.
[41] Hossain, M.A., Pota, H.R., Squartini, S. and Abdou, A.F., 2019. Modified PSO algorithm for real-time energy management in grid-connected microgrids. *Renewable energy*, *136*, pp.746-757.
[42] Naderi, E., Dejamkhooy, A., Seyedshenava, S.J. and Shayeghi, H., 2022. MILP based Optimal Design of Hybrid Microgrid by Considering Statistical Wind Estimation and Demand Response. *Journal of Operation and Automation in Power Engineering*, *10*(1), pp.54-65.